Complex refractive index tunability of graphene at 1550 nm wavelength

F. Xu, S. Das, Y. Gong, Q. Liu, H.-C. Chien, H.-Y. Chiu, J. Wu, and R. Hui

Citation: Applied Physics Letters **106**, 031109 (2015); doi: 10.1063/1.4906349
View online: http://dx.doi.org/10.1063/1.4906349
View Table of Contents: http://scitation.aip.org/content/aip/journal/apl/106/3?ver=pdfcov
Published by the AIP Publishing

Complex refractive index tunability of graphene at 1550 nm wavelength

F. Xu,[1,2] S. Das,[1] Y. Gong,[3] Q. Liu,[3] H.-C. Chien,[3] H.-Y. Chiu,[3] J. Wu,[3] and R. Hui[1]
[1]*Department of Electrical Engineering and Computer Science, The University of Kansas, Lawrence Kansas 66045, USA*
[2]*School of Physics and Materials Science, Anhui University, Hefei 230039, China*
[3]*Department of Physics and Astronomy, The University of Kansas, Lawrence Kansas 66045, USA*

(Received 2 October 2014; accepted 9 January 2015; published online 21 January 2015)

The complex refractive index of graphene fabricated using chemical vapor deposition is characterized at 1550 nm wavelength through the reflectivity measurement on a SiO_2/Si substrate. The observed tunability of the complex reflective index as the function of gate electric voltage is in agreement with the prediction based on the Kubo formula. © *2015 AIP Publishing LLC*.
[http://dx.doi.org/10.1063/1.4906349]

Composed of a single layer of carbon atoms with honeycomb lattice, graphene is a promising two-dimensional material for many potential applications in electronics and photonics. The low-energy band structure of graphene can be described by a pair of Dirac cones.[1,2] At absolute zero temperature, the Fermi energy is at the charge neutrality point (Dirac point) where the lower energy cone is completely filled while the upper one is empty. Owing to the low density of states, the chemical potential in graphene can be modulated by an external gate voltage to populate electrons to the upper cone or deplete electrons from the lower cone. Thus, the tunability of chemical potential is a key to electrically regulating the optical transition of graphene-based devices. The excellent electrical properties of graphene, such as high carrier mobility and electrical conductivity, have been well studied and applied to build high-frequency field-effect transistors (FETs).[3] The unique optical properties of graphene have been applied to create gas sensors,[4] plasmonic resonators in terahertz,[5] and electro-absorption optical modulators at 1550 nm wavelength.[6] Very recently, a variety of graphene based photonic nanostructures and devices have been theoretically proposed for operation in the optical communication wavelengths based on the tunable nature of graphene complex refractive index.[7,8] Thus, to bridge the gap between models and device realization, it is essential to accurately evaluate the refractive index of graphene at 1550 nm wavelength as the function of chemical potential. Most characterizations of graphene dielectric constant have been so far in visible,[9] mid-infrared,[2] and terahertz[5] wavelength ranges. We report here that the voltage-dependent reflectivity at 1550 nm wavelength measured on a back-gated chemical vapor deposition-derived (CVD) graphene on SiO_2/Si substrate is in agreement with the calculated result based on the Kubo formula.[10] Hysteresis of reflectivity in response to the sweep of the applied gate voltage is also observed due to the process of charge trapping and storage in graphene.

Graphene used in this experiment was grown on commercial copper foils with 25 μm thickness (Alfa Aesar, item No. 13382) at ≈1000 °C in a chemical vapor deposition system using a similar procedure as described elsewhere.[11] A mixture of CH_4 (35 sccm) and H_2 (2 sccm) was used as the gas precursors. The Cu foil was heated to the growth temperature of 1000 °C, and then 35 sccm CH_4 was introduced to initiate the graphene growth at a total pressure of 500 mTorr. After 30 min of growth, a continuous monolayer graphene film was grown on the Cu foil. Poly-methyl methacrylate (PMMA) was spin-coated on one side of the as-grown graphene before the sample was immersed into iron chloride solution (0.1 g ml^{-1}) for removal of the copper foil. Graphene films were transferred onto the SiO_2/Si substrates, and the thickness of the SiO_2 layer is 90 nm. Wire bounding was simply made of a small drop of silver paste directly on mm-size CVD graphene to establish the electrical connection through a gold wire. Thus, the electrical potential between graphene and silicon substrate can be varied through the applied gate voltage. The sample was finally placed on an electrically controlled 3D translation stage. Graphene FETs on SiO_2/Si substrates were also fabricated for electrical characterization using procedures reported previously.[12]

Fig. 1 shows the experimental setup. A fiber pigtailed laser diode at 1550 nm wavelength was used in the experiment with spectral linewidth of approximately 10 MHz. The laser output was collimated into the system and focused on the sample through a 20× objective lens, and the spot diameter on the sample was typically about 5 μm. The light reflected from the sample was collected through a 50% beam splitter and detected by a photodetector. A microscope was inserted in the optical system to observe the position of the light spot on graphene sample. A lock-in amplifier was used to improve the signal-to-noise ratio. Optical signal modulation for synchronizing the lock-in amplifier could be applied either through a mechanical chopper in front of the

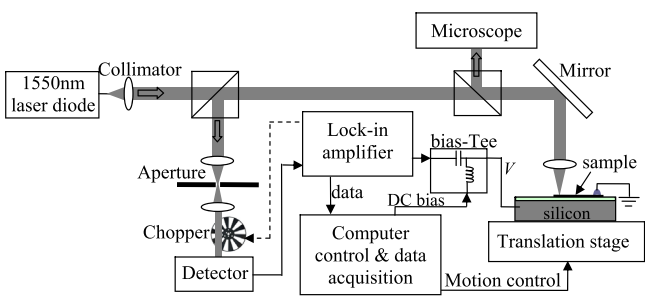

FIG. 1. Experimental setup.

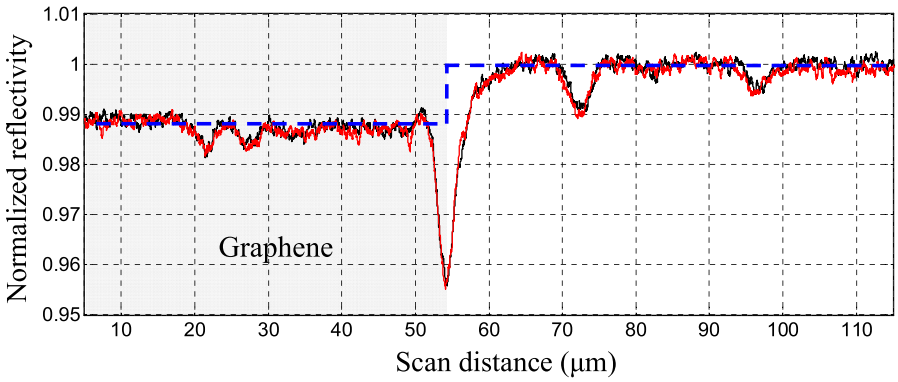

FIG. 2. Normalized power reflectivity from sample surface measured with beam scanning across the edge of single-layer graphene in the forward (red) and backward (black) directions. No gate voltage is applied.

photodetector or through a modulation on the gate voltage of the sample. A computer was used to control the motion of the translation stage, to adjust the gate voltage, and to acquire data from the lock-in amplifier. Fig. 2 shows the normalized reflectivity as the function of the beam position with the laser beam scanning across the edge of the graphene with zero gate voltage. In this measurement, lock-in amplifier was synchronized with the mechanical chopper in front of the photodetector. This allowed the measurement of reflectivity change from the sample surface when the laser beam scanned across areas with and without the graphene, which is approximately 1.1% as shown in Fig. 2. To confirm the repeatability of the measurement, the laser beam was scanned both in the forward and backward directions along the same line, and the results are almost identical. The sharp notch of reflectivity measured at the graphene edge shown in Fig. 2 was attributed to the unavoidable fabrication imperfections to the graphene edges along with the effect of diffraction.

In order to measure the variation of optical power reflectivity R as the function of the applied gate voltage V, the position of the laser beam was fixed on the graphene. As this variation was expected to be less than 1%, the system had to be stable enough, and the impact from laser power variation and interference caused by reflections from various optical components in the system had to be minimized. Thus, in this measurement, instead of using the mechanical chopper, a 5 kHz sinusoid voltage waveform with $2V_{pp}$ amplitude was directly applied on the graphene to synchronize the lock-in amplifier. An adjustable DC gate voltage was added to the small-signal modulating waveform through a bias-tee as illustrated in Fig.1. This is equivalent to a small-signal modulation on chemical potential of the graphene, and therefore the lock-in amplifier actually measures the differential reflectivity $\delta R(V)/\delta V$. Fig. 3 shows the differential reflectivity measured on the graphene when the DC bias voltage was linearly ramped up and down between −20.6 V and 28.6 V, and the rate of this voltage scan was approximately 1.1 V/s. The gate voltage-dependent differential reflectivity shown in Fig. 3 demonstrates the tunability of graphene complex reflectivity, which is clearly not a linear function of the applied gate voltage. The measured $\delta R(V)/\delta V$ characteristics also depend on optical interference of the multi-layered structure of SiO_2/Si substrate. Another observation of Fig. 3 is that $\delta R(V)/\delta V$ depends on the direction of voltage scan, and this hysteresis is attributed to the charge trapping and storage in graphene.

The fundamental optical properties of graphene have been studied theoretically in recent years, and the complex conductivity of graphene can be expressed by the Kubo formula as[10]

$$\sigma(\omega,\mu_c,\Gamma,T)=\frac{je^2(\omega-j2\Gamma)}{\pi\hbar^2}\times\left\{\frac{1}{(\omega-j2\Gamma)^2}\int_0^\infty\varepsilon\left[\frac{\partial f_d(\varepsilon)}{\partial\varepsilon}-\frac{\partial f_d(-\varepsilon)}{\partial\varepsilon}\right]d\varepsilon-\int_0^\infty\left[\frac{f_d(-\varepsilon)-f_d(\varepsilon)}{(\omega-j2\Gamma)^2-4(\varepsilon/\hbar)^2}\right]d\varepsilon\right\},\quad(1)$$

where ω is the optical frequency, e is the electron charge, $\hbar=h/2\pi$ is the reduced Planck's constant, and $f_d(\varepsilon)=1/(e^{(\varepsilon-\mu_c)/k_BT}+1)$ is the Fermi-Dirac distribution function. ε is the energy, k_B is the Boltzmann's constant, T is the temperature, and $\hbar\Gamma=5$ meV is the scattering parameter.[7] μ_c is the chemical potential which is determined by charge accumulation on the graphene. The value of μ_c can be varied by an applied gate voltage V through the silicon oxide capacitance between the graphene and the silicon substrate as

$$\mu_c=\hbar v_F\sqrt{\frac{\pi\varepsilon_{ox}}{ed_{ox}}(V-V_D)},\quad(2)$$

where ε_{ox} and d_{ox} are the dielectric constant and the thickness of SiO_2 layer, and V_D is the Dirac voltage determined by the

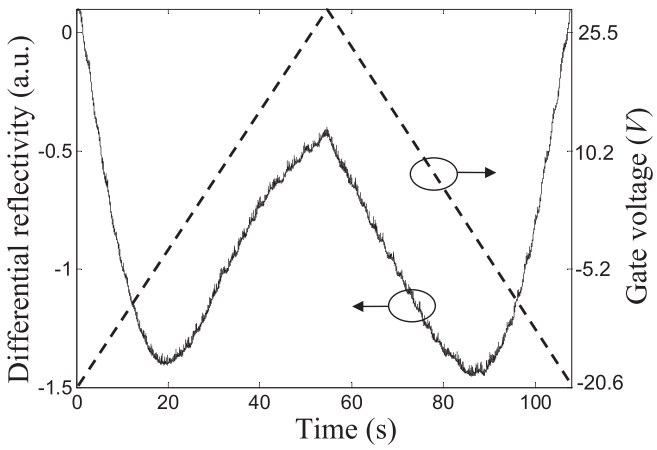

FIG. 3. Measured differential reflectivity (continuous line) and the applied linear scan of gate voltage (dashed line) as the function of time.

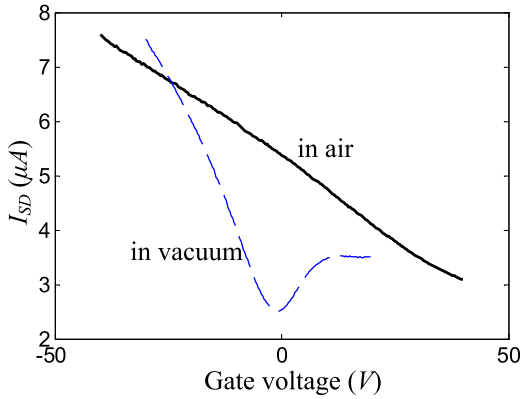

FIG. 4. Source-drain current versus gate voltage curves taken on a representative graphene FET structure in air (solid line) and in vacuum (dashed line).

unintentional doping of the graphene from the substrate and its surrounding environment. $v_F \approx 0.75 \times 10^6$ m/s is the Fermi velocity,[2] which was found to be dependent on the property of the substrate.[13] We observed that when graphene sample was exposed to the open air, V_D might increase dramatically.[11,12] Fig. 4 shows representative curves of source-drain current, I_{SD}, as the function of the gate voltage measured in an FET device made of the same batch of graphene on the SiO_2(90 nm)/Si substrate. Although the V_D value corresponding to the minimum of I_{SD} was approximately zero when the sample was placed in vacuum, V_D moved beyond the measurable voltage window after the sample was exposed to the air. The maximum applicable gate voltage was primarily limited by the practical dielectric strength of silicon oxide of ~0.5 V/nm, corresponding to about ±45 V in this case. Consistent result was obtained on more than 10 similar FETs. Because our optical characterization was performed in the open air under ambient conditions, the Dirac point was expected to be in exceeding 45 V. Raman spectroscopy is widely employed to characterize the structural and electronic properties of graphene materials, including number of layers, stacking order, and band structures, providing information on the tangential *G*-band derived from the in-plane vibration of the sp^2 carbon atoms, the 2*D*-band originated from the two-phonon double resonance, and the disorder-induced *D*-band.[14,15] Fig. 5 shows a typical Raman spectrum of the monolayer graphene films transferred onto the SiO_2/Si substrate (black), and that after

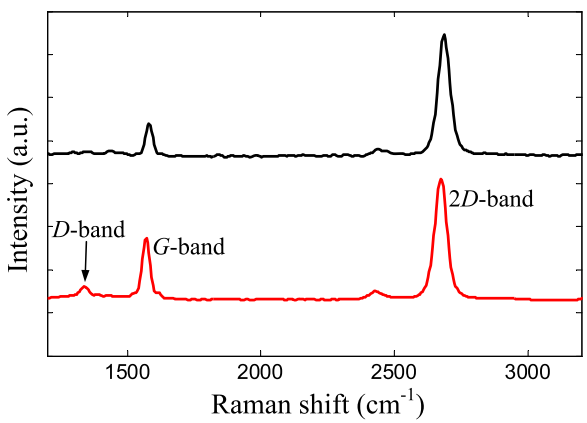

FIG. 5. Measured Raman spectra of the monolayer graphene transferred on the SiO_2/Si substrate (top) and after the electric and optical characterization (bottom). The laser excitation wavelength is 488 nm.

the optical characterization was completed (red). These Raman spectra were taken with a confocal micro-Raman system (WITec, alpha-300) using laser excitation at 488 nm wavelength. On both spectra, two characteristic peaks of graphene, i.e., 2*D*-band at ~2687 cm^{-1} the *G*-band at ~1581 cm^{-1}, are cleanly shown. The high ratio between 2*D*-peak and *G*-peak near or above 2 is the signature of monolayer graphene.[15] *D*-band at ~1349 cm^{-1} is negligible immediately after the graphene transfer (black), which is indicative of the high quality of the monolayer graphene. However, a small *D*-peak with ~7% of magnitude of the intrinsic 2*D*-peak becomes visible after the optical characterization, suggesting that minor damages to graphene may have occurred during electrode deposition and the following characterization of both electric and optical properties, as well as the exposure to open air for an extended period of time.

The conductivity predicted by the Kubo formula[10] can be converted into a complex refractive index as, $n_g = \sqrt{1 - j\sigma/(\omega\varepsilon_0\delta_g)}$, where ε_0 is the free space dielectric constant and $\delta_g = 0.34$ nm is the thickness of a single layer graphene. The normalized change of the power reflectivity on the sample surface without and with the graphene can be calculated based on the multilayer interference theory as[9]

$$\Delta R/R_0 = \pi\delta_g \cdot \mathrm{Re}\{(1 - n_g^2)(1 + r_0)^2/(r_0\lambda)\}, \qquad (3)$$

where r_0 is the optical field reflectivity of the substrate without graphene and λ is the wavelength. For the SiO_2/Si substrate,

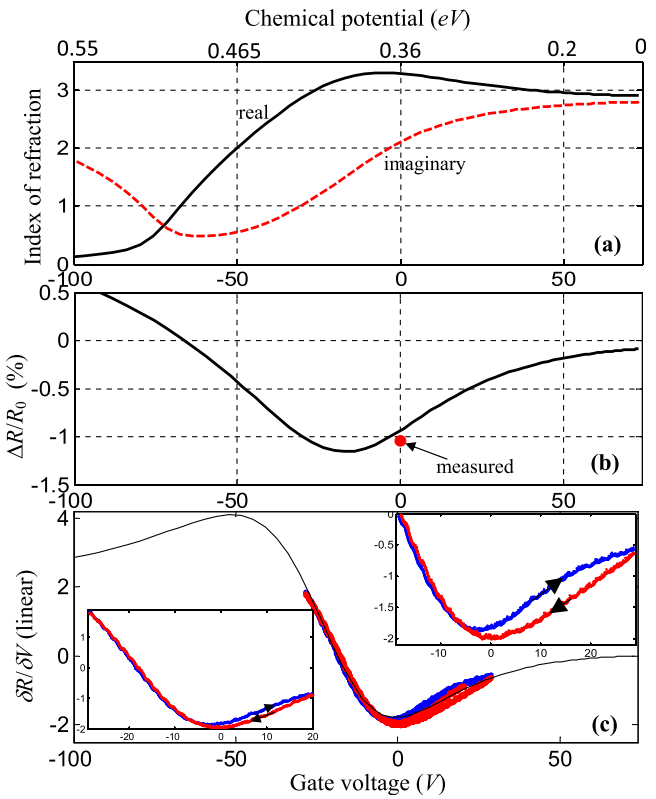

FIG. 6. (a) Calculated complex index based on Kubo formula. (b) Normalized power reflectivity change due to graphene layer on substrate (continuous line) and measured value extracted from Fig. 3. (c) Calculated (continuous line) and measured (dots) differential reflectivity as the functions of chemical potential (top horizontal axis) and gate voltage (bottom horizontal axis). Inset: enlarged views of measured differential reflectivity with different voltage scan windows, indicating hysteresis characteristic.

$r_0 = (r_{01}e^{j\beta_{ox}d_{ox}} + r_{12}e^{-j\beta_{ox}d_{ox}})/(e^{j\beta_1 d_1} + r_{01}r_{12}e^{-j\beta_{ox}d_{ox}})$ and $R_0 = |r_0|^2$, where $\beta_{ox} = 2\pi n_{ox}/\lambda$ is the propagation constant of the oxide layer, and $r_{01} = (n_{ox} - 1)/(n_{ox} + 1)$ and $r_{12} = (n_s - n_{ox})/(n_s + n_{ox})$ are Fresnel reflectivities at air/SiO_2 and SiO_2/Si interfaces, respectively, with n_{ox} and n_s refractive indices of SiO_2 and Si. Fig. 6(a) shows the real and imaginary parts of the graphene refractive index as the function of chemical potential calculated from Eq. (1). The bottom horizontal axis of Fig. 6 indicates the applied gate voltage, which is related to the chemical potential through Eq. (2). We used $V_D = 74$ V and $d_{ox} = 95$ nm to obtain the best fit to the measured results. The solid line in Fig. 6(b) is the graphene induced power reflectivity change calculated from Eq. (3), and the solid dot indicates $\Delta R/R_0 = 1.1\%$ at the gate voltage $V = 0$, as shown in Fig. 2. The continuous line in Fig. 6(c) shows the calculated differential reflectivity $\delta R(V)/\delta V$, which is the derivative of the solid line in Fig. 6(b). Dotted lines in Fig. 6(c) are $\delta R(V)/\delta V$ measured with linear scanning of the gate voltage V, and the results agree reasonably well with the calculated values, except for the apparent hysteresis in the measured curves that are not considered in the theoretical model. The insets in Fig. 6(c) show enlarged views of the measured differential reflectivity R for the gate voltage scan between −29 V and +20 V (bottom left), and between −20 V and +29 V (top right). Hysteresis is clearly shown in both of the two measurements, indicating different reflectivity changes corresponding to the ramp-up and ramp-down process of the applied voltage. The hysteresis loop is wider when the graphene is biased closer to the Dirac point. The characteristic of hysteresis has been previously reported in gate voltage dependent I_{SD} in graphene-based FET structures,[16,17] but not for the optical properties such as the change of power reflectivity. This effect has to be considered in the design and application of graphene based photonic devices.

In summary, the reflectivity variation across the edge of CVD graphene on a SiO_2(90 nm)/Si substrate was measured at 1550 nm optical communications wavelength. The measured change of reflectivity as the function of applied gate voltage agrees reasonably well with the theoretical prediction based on modeling using the Kubo formula. This verifies the tunability of complex refractive index of graphene, which is the most important parameter for the design of graphene based photonic devices for optical communications.

The authors acknowledge support in part by ARO Contract Nos. AROW911NF-09–1–0295 and W911NF-12-1-0412, NSF Contract Nos. NSF-DMR-1105986 and NSF EPSCoR-0903806, and matching support from the State of Kansas through Kansas Technology Enterprise Corporation.

[1]J. Horng, C.-F. Chen, B. Geng, C. Girit, Y. Zhang, Z. Hao, H. A. Bechtel, M. Martin, A. Zettl, M. F. Crommie, Y. R. Shen, and F. Wang, "Drude conductivity of Dirac fermions in graphene," Phys. Rev. B **83**, 165113 (2011).
[2]F. Wang, Y. Zhang, C. Tian, C. Girit, A. Zettl, M. Crommie, and Y. R. Shen, "Gate-variable optical transitions in graphene," Science **320**, 206–209 (2008).
[3]Y.-M. Lin, C. Dimitrakopoulos, K. A. Jenkins, D. B. Farmer, H.-Y. Chiu, A. Grill, and Ph. Avouris, "100-GHz transistors from wafer-scale epitaxial graphene," Science **327**, 662 (2010).
[4]F. Schedin, A. K. Geim, S. V. Morozov, E. W. Hill, P. Blake, M. I. Katsnelson, and K. S. Novoselov, "Detection of individual gas molecules adsorbed on graphene," Nat. Mater. **6**, 652–655 (2007).
[5]L. Ju, B. Geng, J. Horng, C. Girit, M. Martin, Z. Hao, H. A. Bechtel, X. Liang, A. Zettl, Y. R. Shen, and F. Wang, "Graphene plasmonics for tunable terahertz metamaterials," Nat. Nanotechnol. **6**, 630–634 (2011).
[6]M. Liu, X. Yin, E. Ulin-Avila, B. Geng, T. Zentgraf, L. Ju, F. Wang, and X. Zhang, "A graphene-based broadband optical modulator," Nature **474**, 64–67 (2011).
[7]Z. Lu and W. Zhao, "Nanoscale electro-optic modulators based on graphene-slot waveguides," J. Opt. Soc. Am. B **29**, 1490–1496 (2012).
[8]L. Yang, T. Hu, A. Shen, C. Pei, B. Yang, T. Dai, H. Yu, Y. Li, X. Jiang, and J. Yang, "Ultracompact optical modulator based on graphene-silica metamaterial," Opt. Lett. **39**, 1909–1912 (2014).
[9]X. Wang, Y. P. Chen, and D. D. Nolte, "Strong anomalous optical dispersion of graphene: Complex refractive index measured by picometrology," Opt. Express **16**, 22105 (2008).
[10]G. W. Hanson, "Dyadic Green's functions and guided surface waves for a surface conductivity model of graphene," J. Appl. Phys **103**, 064302 (2008).
[11]J. Liu, G. Xu, C. Rochford, R. Lu, J. Wu, C. M. Edwards, C. L. Berrie, Z. Chen, and V. A. Maroni, "Doped graphene nanohole arrays for flexible transparent conductors," Appl. Phys. Lett **99**, 023111 (2011).
[12]G. Xu, R. Lu, J. Liu, H. Chiu, R. Hui, and J. Wu, "Photodetection based on ionic liquid gated plasmonic Ag nanoparticle/graphene nanohybrid field effect transistors," Adv. Opt. Mater. **2**, 729–736 (2014).
[13]C. Hwang, D. A. Siegel, S.-K. Mo, W. Regan, A. Ismach, Y. Zhang, A. Zettl, and A. Lanzara, "Fermi velocity engineering in graphene by substrate modification," Sci. Rep. **2**, 590 (2012).
[14]Z. H. Ni, Y. Y. Wang, T. Yu, and Z. X. Shen, "Raman spectroscopy and imaging of graphene," Nano Res. **1**, 273–291 (2008).
[15]A. Gupta, G. Chen, P. Joshi, S. Tadigadapa, and P. C. Eklund, "Raman scattering from high-frequency phonons in supported n-graphene layer films," Nano Lett. **6**, 2667–2673 (2006).
[16]Y. G. Lee, C. G. Kang, U. J. Jung, J. J. Kim, H. J. Hwang, H.-J. Chung, S. Seo, R. Choi, and B. H. Lee, "Fast transient charging at the graphene/SiO_2 interface causing hysteretic device characteristics," Appl. Phys. Lett. **98**, 183508 (2011).
[17]H. Kalita, V. Harikrishnan, D. B. Shinde, V. K. Pillai, and M. Aslam, "Hysteresis and charge trapping in graphene quantum dots," Appl. Phys. Lett. **102**, 143104 (2013).